JOURNAL OF BONE AND MINERAL RESEARCH
Volume 24, Number 9, 2009
Published online on March 30, 2009; doi: 10.1359/JBMR.090317

Role of Trabecular Microarchitecture in Whole-Vertebral Body Biomechanical Behavior

Aaron J. Fields,[1] Senthil K. Eswaran,[1] Michael G. Jekir,[1] and Tony M. Keaveny[1,2]

ABSTRACT: The role of trabecular microarchitecture in whole-vertebral biomechanical behavior remains unclear, and its influence may be obscured by such factors as overall bone mass, bone geometry, and the presence of the cortical shell. To address this issue, 22 human T_9 vertebral bodies (11 female; 11 male; age range: 53–97 yr, 81.5 ± 9.6 yr) were scanned with μCT and analyzed for measures of trabecular microarchitecture, BMC, cross-sectional area, and cortical thickness. Sixteen of the vertebrae were biomechanically tested to measure compressive strength. To estimate vertebral compressive stiffness with and without the cortical shell for all 22 vertebrae, two high-resolution finite element models per specimen—one intact model and one with the shell removed—were created from the μCT scans and virtually compressed. Results indicated that BMC and the structural model index (SMI) were the individual parameters most highly associated with strength (R^2 = 0.57 each). Adding microarchitecture variables to BMC in a stepwise multiple regression model improved this association (R^2 = 0.85). However, the microarchitecture variables in that regression model (degree of anisotropy, bone volume fraction) differed from those when BMC was not included in the model (SMI, mean trabecular thickness), and the association was slightly weaker for the latter (R^2 = 0.76). The finite element results indicated that the physical presence of the cortical shell did not alter the relationships between microarchitecture and vertebral stiffness. We conclude that trabecular microarchitecture is associated with whole-vertebral biomechanical behavior and that the role of microarchitecture is mediated by BMC but not by the cortical shell.
J Bone Miner Res 2009;24:1523–1530. Published online on March 30, 2009; doi: 10.1359/JBMR.090317

Key words: trabecular microarchitecture, osteoporosis, spine, biomechanics, vertebral strength

Address correspondence to: *Aaron J. Fields, MS, 2166 Etcheverry Hall, University of California, Berkeley, CA 94720-1740, USA, E-mail: afields@me.berkeley.edu*

INTRODUCTION

The inability of DXA to accurately predict osteoporotic fractures[1] or fully account for decreases in fracture risk associated with antiresorptive treatment[2,3] has magnified clinical interest in parameters related to bone quality.[4,5] Of particular interest is trabecular microarchitecture, given its important role in the mechanical behavior of isolated specimens of trabecular bone.[6–9] However, the influence of trabecular microarchitecture on whole-vertebral strength and stiffness is not well understood and may be obscured by potentially dominant morphological factors such as vertebral size, vertebral shape, overall bone mass, and the presence of the cortical shell. Understanding the relationships between microarchitectural and morphological indices and the biomechanical properties of the human vertebral body may therefore help elucidate the mechanisms by which trabecular microarchitecture contributes to vertebral fracture etiology.

Several factors contribute to a vertebra's biomechanical behavior, including BMC and BMD,[10–13] cortical shell thickness,[14] and geometric size and shape.[15] Despite the fact that the trabecular bone in the anterior and superior regions of the lumbar vertebra is less dense and connected than in the posterior and inferior regions,[16,17] it was recently reported that vertebral strength could not be explained through microarchitecture analysis of one specific region.[17] This raises questions about possible interaction effects between trabecular microarchitecture, the cortical shell—which has a substantial and complex load-bearing role in the human vertebra[14,18,19]—and vertebra size (reflected in part by overall bone mass) in terms of contributions to vertebral strength. It is possible, for example, that the role of trabecular microarchitecture in vertebral strength is influenced by the cortical shell or by bone mass.

The overall goal of this study was to investigate the role of trabecular microarchitecture in whole-vertebral biomechanical behavior, accounting also for such factors as vertebral mass, cortical shell morphology, and indeed the presence of the cortical shell itself. We addressed this issue using a combination of cadaver biomechanical testing, high-resolution μCT imaging, and μCT-based finite element modeling. Specifically, our objectives were to (1)

Dr. Keaveny holds equity interests in O.N. Diagnostics. All other authors state that they have no conflicts of interest.

[1]Orthopaedic Biomechanics Laboratory, Department of Mechanical Engineering, University of California, Berkeley, California, USA; [2]Department of Bioengineering, University of California, Berkeley, California, USA.

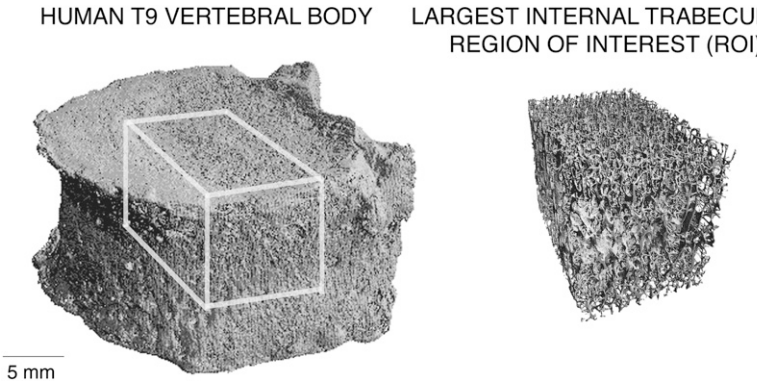

FIG. 1. Example μCT rendering of a human T_9 vertebral body (left) with largest internal cuboid of trabecular bone isolated for microarchitecture analysis (right).

assess the individual effects of trabecular microarchitecture, cortical shell thickness, vertebral cross-sectional area (CSA), and bone mass on vertebral strength and stiffness; (2) determine the combined effects of these parameters on vertebral strength and stiffness; and (3) determine whether the physical presence of the shell alters the relation between trabecular microarchitecture and vertebral stiffness. This study is the first to relate the individual and combined effects of vertebral morphology, trabecular microarchitecture, cortical morphology, and the presence of the cortical shell to the biomechanical behavior in which all assays are performed on the same human vertebrae.

MATERIALS AND METHODS

Fresh-frozen human spine segments were obtained from willed-body programs subject to exclusion of any donors having a documented history of metabolic bone disease (e.g., metastatic cancer or hyper- and hypothyroidism). Anterior–posterior and lateral view radiographs of accepted specimens were examined (M.G.J.) to identify and exclude any T_9 vertebrae showing evidence of preexisting vertebral fractures or scoliosis. Twenty-two T_9 vertebrae ($n = 11$ male; $n = 11$ female; age range: 53–97 yr, mean ± SD = 81.5 ± 9.6 yr) were thus obtained.

After removing the posterior elements, each isolated T_9 vertebral body was μCT scanned using a 30-μm voxel size (Scanco 80; Scanco Medical, Brüttisellen, Switzerland), and a number of bone morphology and microarchitecture variables were measured from these scans. BMC for each vertebra was estimated based on the measured bone volume and the assumption of constant tissue density (2.05 g/ml[20]), a technique that performs well compared with DXA-derived BMC.[21] Model-independent trabecular microarchitecture parameters were measured for the largest internal cuboid region of trabecular bone, typically ~15 × 15 × 10 mm (Fig. 1). The microarchitecture variables studied were measured using the Scanco software and comprised bone volume fraction (BV/TV), mean trabecular thickness (Tb.Th), mean trabecular number (Tb.N), mean trabecular separation (Tb.Sp), structural model index (SMI),[22] connectivity density (Conn.D),[23] and degree of anisotropy (DA).

To characterize biomechanical properties, destructive compressive tests were performed after μCT scanning for a subset of 16 specimens ($n = 10$ male; $n = 6$ female; age range: 53–97 yr, 77.5 ± 10.1 yr; the remaining six vertebrae were unavailable because they were used in a different type of biomechanical testing experiment). The specimens were cleared of soft tissues, placed between molds of polymethylmethacrylate (PMMA) bone cement to ensure plano-parallel ends,[24–26] and tested at room temperature to failure in displacement control at either 0.50[26] or 0.06% strain/s[27] after preconditioning[26]. Saline-soaked gauze was used to keep the samples moist throughout the experiments. Our main outcome parameter, vertebral strength (F_{ult}), was defined as the peak force achieved during the loading cycle,[26] which occurred typically at a strain of ~1.8%. Vertebral stiffness was not measured because we did not use specimen-attached extensometers, and thus machine compliance effects would confound the resulting deformation measures. Although the strength behavior of both cortical and trabecular bone depend on strain rate when strain rate is varied over many orders of magnitude,[28,29] the effect of strain rate is negligible in the range used here ($p = 0.91$; 0.1 versus 1.0% strain/s[28]). Thus, our data were not adjusted for any differences in applied strain rate.

In addition to this biomechanical testing, we performed finite element (FE) analysis on each of the $n = 22$ specimens to estimate vertebral compressive stiffness with and without the cortical shell. For each vertebra, two FE models—one intact and one with the cortical shell virtually removed—were created using previously reported methods.[14,30,31] Briefly, the scans were region-averaged to 60-μm voxel size and segmented using a global threshold value. A custom algorithm (IDL 6.2; ITT Visual Information Solutions, Boulder, CO, USA) using moving averages[14,30] was used to identify the cortical shell. Each 60-μm cubic voxel was converted into an eight-noded element to create an FE model of the entire vertebral body. Because the cortical shell is often described as condensed trabeculae,[32–34] all cortical and trabecular bone elements in the models were assigned the same hard tissue properties (elastic modulus 18.5 GPa and Poisson's ratio of 0.3). Polymethylmethacrylate (elastic modulus 2.5 GPa and Poisson's ratio of 0.3[35]) layers were added to the inferior and superior endplates of the vertebral body to mimic experiments. To determine how the presence of the shell influences the role of trabecular microarchitecture

TABLE 1. Donor, Whole Bone Mophometry, Cortical Shell, Trabecular Microarchitecture, and Biomechanical Data for the 22 Human T_9 Vertebral Bodies Included in This Study

	Mean	*SD*	*CV* (%)*	*Range*
Donor				
Age (yr)	81.5	9.6	11.8	53–97
Body mass (kg)	59.9	12.2	20.3	38.6–86.4
Whole bone morphology				
BMC (g)	8.16	3.01	36.9	3.7–13.5
CSA (cm^2)	8.49	1.59	18.7	5.8–11.3
Cortical shell				
Ct.Th (mm)	0.38	0.09	24.5	0.25–0.54
Ct.M (%)	14.5	3.3	22.9	8.9–21.5
Trabecular microarchitecture				
BV/TV (%)	9.8	1.8	18.9	7.2–14.1
Tb.N (mm^{-1})	0.99	0.10	10.3	0.78–1.14
Tb.Sp (mm)	0.98	0.11	11.5	0.82–1.21
Tb.Th (mm)	0.16	0.02	13.8	0.12–0.22
DA	1.42	0.08	5.7	1.27–1.60
Conn.D (mm^{-3})	3.02	0.80	26.6	1.16–4.48
SMI	2.19	0.30	13.6	1.34–2.72
Biomechanical properties				
Vertebral strength, F_{ult} (N)†	3250	1420	43.7	1420–6570
Vertebral stiffness, K_{intact} (kN/mm)	44.9	17.6	39.2	19.4–79.6
Trabecular stiffness, K_{trab} (kN/mm)	26.4	13.7	51.9	8.4–57.1
K_{trab}/K_{intact} (%)	56.6	10.8	19.1	35.7–73.2

* CV = SD/mean.

† Vertebral strength measured only for 16 vertebrae.

in vertebral biomechanical behavior, a second FE model without the cortical shell was created for each specimen, and stiffness was computed for this model while keeping all other model inputs the same as in the intact model.

The resulting FE models had up to 80 million elements and >300 million degrees of freedom and required highly specialized software and hardware for analysis.[36] To simulate compressive loading, the superior surface of each model was displaced to 1.0% apparent level strain in the inferior–superior direction. The inferior surface was fixed to mimic experimental testing protocols. All analyses were run using custom code—including parallel mesh partitioner and algebraic multigrid solver[36]—on an IBM Power4 supercomputer (Datastar, San Diego, CA, USA) and required a maximum of 880 processors in parallel and 1800 GB of memory. These analyses provided a number of outcome parameters. Vertebral stiffness (K_{intact}) was defined as the ratio of the reaction force generated at the inferior surface to the applied displacement. A similar calculation was used to define the stiffness of the trabecular compartment (K_{trab}) but using instead the results from the vertebra model without the shell. The contribution of the trabecular compartment to whole-vertebral stiffness, an indicator of load sharing between the cortical and trabecular bone, was quantified by the ratio K_{trab}/K_{intact}. The region-averaged 60-μm models were also used to calculate the average thickness of the cortical shell (Ct.Th) in the transverse region excluding the endplates,[14] as well as a ratio of cortical shell mass to whole bone mass—cortical mass fraction (Ct.M). Minimum vertebral CSA was determined using a moving average for 1-mm-thick transverse slices.

The independent roles of trabecular microarchitecture, cortical shell thickness, and vertebral morphology in the biomechanical outcomes were quantified by the Pearson correlation coefficient. All explanatory variables were also correlated with each other to explore cross-correlation effects. The combined roles of trabecular microarchitecture, morphology, and BMC in strength and stiffness were quantified using stepwise multiple linear regressions (JMP 7.0; SAS Institute, Cary, NC, USA), which sequentially add the most significant explanatory variable to the model until the unexplained variability in the dependent parameter cannot be reduced. To determine whether the presence of the cortical shell alters the role of microarchitecture, stiffness–architecture relationships were determined using intact and trabecular stiffness as the outcome. The statistically significant intact and trabecular stiffness–architecture relationships were compared using a *t*-test on the regression slopes. All regressions and tests were taken as significant at $p < 0.05$.

RESULTS

The average value of bone volume fraction was <10% (Table 1), indicating the low-density nature of the vertebrae analyzed. Consistent with this, strength values (1420–6570 N) were typical of an elderly cohort with low bone mass.[10]

Of all measured explanatory variables, BMC ($r = 0.76$) and SMI ($r = -0.76$) showed the highest associations with vertebral strength, whereas BMC was most highly associated with vertebral stiffness ($r = 0.90$; Table 2). Overall, the remaining trabecular microarchitecture parameters showed modest correlations with either vertebral strength

TABLE 2. Independent Role (Pearson's Correlation Coefficient, r) of Trabecular Microarchitecture, Cortical Shell Thickness, and Vertebral Morphology on Biomechanical Properties (n = 22, Unless Noted)

	BMC	*CSA*	*Ct.Th*	*Ct.M*	*BV/TV*	*Tb.N*	*Tb.Sp*	*Tb.Th*	*DA*	*Conn.D*	*SMI*
F_{ult}*	0.76†	0.48	0.50‡	−0.45	0.66§	−0.28	0.21	0.31	0.46	−0.35	−0.76†
K_{intact}	0.90†	0.66†	0.66†	−0.49‡	0.61§	−0.36	0.28	0.39	0.35	−0.38	−0.67†
K_{trab}	0.87†	0.69†	0.46‡	−0.64§	0.62§	−0.31	0.24	0.33	0.35	−0.31	−0.73†
K_{trab}/K_{intact}	0.53‡	0.50‡	−0.10	−0.85†	0.40	−0.02	<0.01	0.01	0.13	0.07	−0.54§

* Vertebral strength measured only for 16 vertebrae.
† $p < 0.001$.
‡ $p < 0.05$.
§ $p < 0.01$.

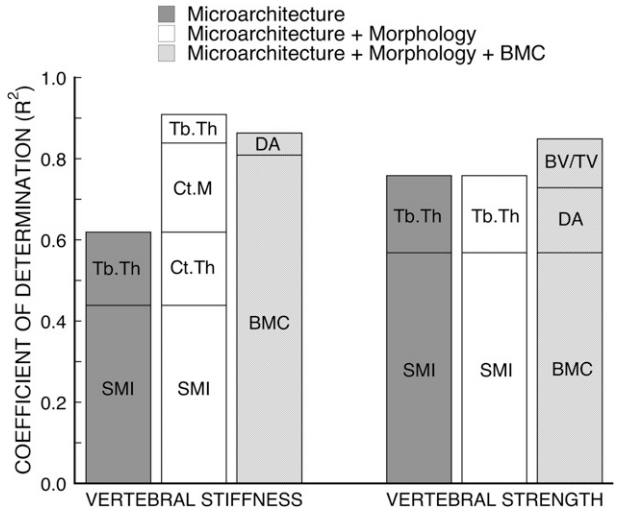

FIG. 2. R^2 values for combined contributions of microarchitecture, morphology, and BMC in stepwise multiple regression models for FE-predicted vertebral stiffness (n = 22) and experimentally measured vertebral strength (n = 16). Microarchitecture considers all BV/TV, Tb.N, Tb.Sp, Tb.Th, DA, Conn.D, and SMI. Morphology considers all CSA, Ct.Th, and Ct.M. See text for nomenclature.

or stiffness ($|r|$= 0.21–0.66), with significant correlations only occurring for SMI and BV/TV. As expected from previous studies,[37] FE-computed whole–vertebral stiffness and compression test–measured vertebral strength were highly correlated (r = 0.87). Vertebral strength and stiffness were weakly correlated with donor age (r = −0.50 and r = −0.66, respectively) but not with donor body mass.

Results from the multiple regression analyses indicated that trabecular microarchitecture was strongly associated with vertebral strength and stiffness, but its role was mediated by BMC (Fig. 2). Combined measures of trabecular microarchitecture (SMI and Tb.Th)—when considered without data on BMC and cortical morphology—could explain an appreciable degree of variability in vertebral strength (R^2 = 0.76) and stiffness (R^2 = 0.62). However, when BMC was added to the model, the architecture variables in the multiple regression model changed (strength: DA and BV/TV; stiffness: DA) and the degree of correlation increased (strength and stiffness: R^2 = 0.85). Scatterplots of the regression models with BMC alone and with BMC plus microarchitecture as predictors of vertebral strength (Fig. 3) and a comparison between the changes in the residuals for the weaker one half (n = 8) versus the stronger one half (n = 8) of the specimens showed significantly greater reductions for the weaker group (Wilcoxon rank–sum test, p = 0.04). This indicates that including microarchitecture parameters in the model had a greater effect on the low-strength specimens. Variations in cortical morphology were not associated with vertebral strength after accounting for either microarchitecture or BMC.

One-way correlations between the explanatory variables showed a number of moderately strong cross-correlation effects (Table 3). For example, BMC was correlated ($|r| >$ ~0.5) with the structure and density of trabecular bone (SMI and BV/TV, respectively), cortical shell morphology (Ct.Th and Ct.M), and vertebral size (CSA).

Relationships between each of the microarchitecture parameters and vertebral stiffness with the shell removed were similar to those with intact vertebral stiffness (t-test on regression slopes, p = 0.09–0.63), indicating that the physical presence of the cortical shell did not alter the relationships between trabecular microarchitecture and vertebral stiffness. The unique mechanical contribution of the trabecular bone, K_{trab}/K_{intact}, varied from 36% to 73% of the intact vertebral stiffness and was most significantly associated with the relative amounts of cortical and trabecular bone (Ct.M, r = −0.85). Of the microarchitecture parameters, there was an association between the stiffness contribution of the trabecular compartment and the plate-like nature of the trabeculae (SMI, r = −0.54).

DISCUSSION

Taken together, these results showed that trabecular microarchitecture was associated with vertebral strength and that its role was mediated by bone mass but not by CSA or the cortical shell. This mediation effect was caused in part by significant cross-correlations between bone mass and trabecular microarchitecture. As a result of these cross-correlation effects, different microarchitecture parameters were associated with measured vertebral strength when included in a multiple regression model with bone mass (DA and BV/TV) than when included in a model without bone mass (SMI and Tb.Th). Bone volume fraction is related to porosity (=1 − BV/TV) and can be considered a surrogate of volumetric bone density rather than a strict measure of microarchitecture. Thus, whereas SMI and Tb.Th together seem to be the most important microarchitecture parameters when bone mass and

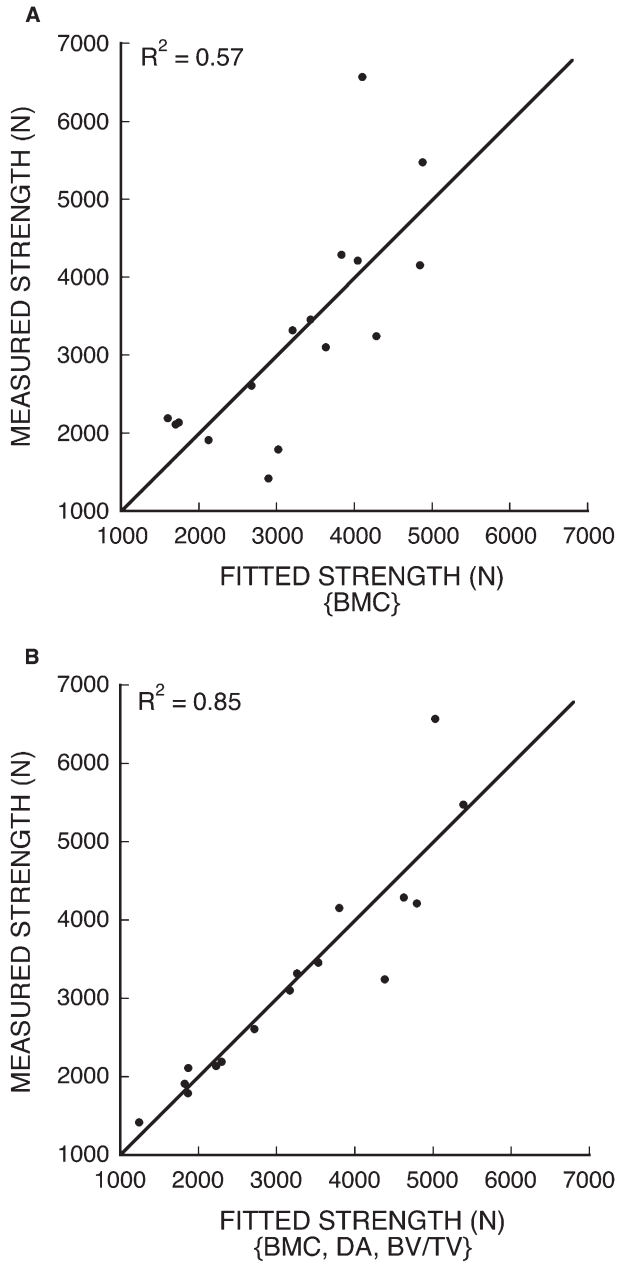

FIG. 3. Fitted vs. measured vertebral strength. (A) BMC as a single predictor of strength (Strength = BMC × 376 – 196). (B) BMC, DA, and BV/TV as predictors of strength (Strength = BMC × 244 + DA × 7660 + BV/TV × 29,700 – 12,900).

trabecular density are not available, the degree of anisotropy seems to be the most important microarchitecture parameter when bone mass and density data are available. Furthermore, our findings suggest that the role of microarchitecture may be more important in low-strength vertebrae.

One unique feature of this study was our use of the FE modeling technique to virtually remove the cortical shell—a task that would have been difficult to perform experimentally—to test whether its physical presence alters the role of trabecular microarchitecture on whole-vertebral stiffness. This provided mechanistic insight into the multiple regression analyses. We also performed all assays on the same specimens, thereby eliminating scatter caused by the use of neighboring vertebrae or peripheral sites for microarchitecture and biomechanical analyses. In addition, model-independent microarchitecture parameters were determined from μCT scans at 30-μm resolution to reduce partial volume effects on measurement accuracy.[38] In terms of external validity, this elderly cohort spanned a range of equivalent QCT-BMD values for trabecular bone (determined using a linear relationship between apparent density and QCT-BMD[39]) both above (n = 11) and below (n = 11) a reported clinical fracture threshold of 110 mg/ml,[40] and thus represented a population at risk for vertebral fracture.

The most important limitation of this study was the modest sample size, which may prevent the extension of our findings to a wider range of bone phenotypes, including younger individuals with higher bone volume fractions. Additionally, the loading conditions used for the biomechanical assays were chosen to provide controlled boundary conditions common in laboratory cadaver testing, but as a result were not fully representative of in vivo loading. Under more physiological loading conditions, the endplates should experience larger strains than those observed here,[31,41] and thus it is not clear how our results would change if the vertebrae were compressed by intervertebral discs. However, a previous study[17] on functional spine units (which allowed loading by a disc) reported only a moderate correlation (R^2 = 0.38; p = 0.003) between yield strength and endplate thickness. Moreover, because the cortical shell is loaded less during compression through the disc, the role of the shell in vertebral strength, including any tendency to obscure trabecular contributions, may be even smaller than reported here. Associated with this issue is the effect of any added bending moment—possibly arising as a result of forward flexion—on the relative contributions of the trabecular and cortical compartments compared with the case of uniform compression. Although in vivo loads on the vertebral body during flexed postures are not well understood, preliminary studies suggest peripheral bone has a greater role under bending loads[42] and that less optimal stress transfer may occur in osteoporotic trabecular bone.[19] Further study is needed to address this issue.

A more technical caveat of our approach is that the absence of stiffness data from the mechanical tests prevented us from correlating FE predictions with experimental results. Unlike in our models, stiffness is difficult to measure in the experiments for several reasons. First, the force–deformation curve is not linear; therefore, experimental measures of stiffness are highly sensitive to the region of the curve analyzed. Second, because of machine compliance and the possible presence of soft tissue or gaps between the PMMA and endplates, stiffness measured from cross-head displacement is not reflective of the actual stiffness of the vertebra—a challenge because the FE models contain an idealized interface between the PMMA and bone. However, the high correlation between FE-predicted and experimentally measured stiffness[7] found previously for trabecular cores lends support to the validity

TABLE 3. Pearson's Correlation Coefficient (r) Between BMC, Trabecular Microarchitecture, and Morphological Parameters as Measured by μCT (n = 22)

	BMC	*CSA*	*Ct.Th*	*Ct.M*	*BV/TV*	*Tb.N*	*Tb.Sp*	*Tb.Th*	*DA*	*Conn.D*
BMC	—									
CSA	0.83*	—								
Ct.Th	0.66*	0.33	—							
Ct.M	−0.48†	−0.44†	0.16	—						
BV/TV	0.58‡	0.31†	0.50†	−0.17	—					
Tb.N	−0.23	−0.34	−0.10	0.08	0.28	—				
Tb.Sp	0.19	0.34	0.06	−0.06	−0.37	−0.98*	—			
Tb.Th	0.30	0.29	0.28	0.07	0.29	−0.52†	0.45†	—		
DA	0.18	0.06	0.08	−0.24	−0.05	−0.69*	0.65*	0.45†	—	
Conn.D	−0.26	−0.32	−0.21	< 0.01	0.10	0.91*	−0.85*	−0.71*	−0.76*	—
SMI	−0.65‡	−0.47†	−0.42	0.34	−0.69*	0.11	−0.08	0.04	−0.19	0.08

* $p < 0.001$.
† $p < 0.05$.
‡ $p < 0.01$.

of our models. Additionally, element size was determined from a numerical convergence analysis.[14] Because we applied the same linear modeling technique to all specimens, relative predictions of stiffness and the role of microarchitecture should be robust.

One clinical limitation is that a lack of DXA or QCT data for this cohort did not allow us to compare against those modalities. At the time of these scans, we did not have a standard calibration of the tissue density detected by the μCT scanner. However, a recent study comparing DXA-derived BMC with μCT estimates using the assumption of constant tissue density showed excellent agreement (R^2 = 0.96, slope of 1) between these two techniques.[21] Moreover, the CV in mean tissue mineral density for human trabecular bone is <2.1%,[43] and thus, the error in BMC estimates associated with our assumption of constant tissue density should not be appreciable. Because we did not have DXA scans, we have no information on the role of microarchitecture in the presence of DXA-derived areal BMD data for the spine. Clinically, such BMD data would likely be combined with trabecular microarchitecture measurements from the spine or from peripheral sites, both at lower resolutions. Our findings are consistent with results from a previous study that found trabecular microarchitecture parameters in the spine, particularly SMI and BV/TV, were highly indicative of vertebral fracture risk.[44] At peripheral sites, trabecular microarchitecture is weakly correlated with that of the spine,[45] and clinical studies using architecture from peripheral sites to differentiate vertebral fracture patients from nonfracture controls have had mixed success.[46,47] Additional research is needed to elucidate the role of microarchitecture from peripheral sites in vertebral fracture risk.

The results of this study are consistent with and complementary to previous studies on the role of microarchitecture in vertebral strength,[17,21,48] and taken together, suggest that improvements in vertebral strength prediction are best achieved through considering the trabecular microarchitecture of the vertebra of interest. One-way strength–architecture relationships were in close agreement with those found by others,[17] indicating that a vertebra's strength does indeed depend on its trabecular microarchitecture. However, the role of trabecular microarchitecture was only marginal in the strength of a neighboring vertebra.[48] These results can thus be thought of as a best-case scenario for the use of microarchitecture measures to predict vertebral strength. Volume fraction accounts for the fact that larger vertebrae are less dense than smaller specimens with the same BMC; after bone size and quantity effects, the remaining differences in vertebral strength were most significantly associated with variations in the degree of trabecular anisotropy. Pooled results from a recent monkey study showed a comparable increase (from 67% to 88%) in prediction of measured strength by including Tb.Sp, SMI, and bone surface-to-volume ratio with BMC of the same specimens.[21] Bone volume fractions were ~26–32% in that study. It remains to be seen whether the microarchitecture parameters most associated with human vertebral strength after accounting for bone mass are the same for both low- and high-density vertebrae.

Our results showed that the physical presence of the shell does not seem to change the role of trabecular microarchitecture in vertebral stiffness. One implication of this unexpected result is that the insight gained from studying the effects of microarchitecture in isolated specimens of trabecular bone may extend to whole-vertebral behavior. Along with the stiffness–architecture relationships, strength–architecture relationships may too be unaffected by the presence of the shell because microarchitecture and cortical morphology had similar independent effects on both vertebral stiffness and strength. Another interesting finding was that cortical morphology was not associated with vertebral strength in multiple regression. One hypothesis is that the failure behavior of the vertebra is more sensitive to differences in trabecular microarchitecture that reflect the bone's susceptibility to buckling (e.g., Tb.Th and SMI)[49] rather than to differences in cortical shell morphology. Given the shell's substantial contribution to vertebral strength[50,51] and stiffness[14,19,30] and that a recent clinical study using FE analysis of QCT scans indicated a potentially important role of the peripheral bone on vertebral fracture risk,[46] further research is recommended into the independent role of the cortical shell for vertebral strength prediction and clinical fracture risk assessment. These data

are not inconsistent with those findings; instead, they suggest that the roles of the cortical shell and trabecular microarchitecture are largely independent. We also note that the plate-like nature of the trabeculae was individually predictive of the stiffness contribution of the trabecular compartment (K_{trab}/K_{intact}) but that the effect was secondary compared with the relative mass of the cortical and trabecular bone. Whereas this supports the argument that compressive load sharing may primarily involve vertically aligned bone tissue,[30] additional research is needed to understand the contributions of horizontal and vertical trabeculae to whole-vertebral biomechanical behavior.[52]

In summary, our findings show that trabecular microarchitecture was associated with whole-vertebral biomechanical behavior and that its role was mediated by BMC but not by vertebral CSA or the cortical shell. Furthermore, it seems that the role of trabecular microarchitecture, when considered in conjunction with information on bone mass and density, was more accentuated in low-strength vertebrae and involves mostly the degree of anisotropy.

ACKNOWLEDGMENTS

Funding was provided by the National Institutes of Health (Grant AR49828). Computational resources were available through Grant UCB-266 from the National Partnership for Advanced Computational nfrastructure. All finite element analyses were performed on an IBM Power4 supercomputer (Datastar, San Diego Supercomputer Center). Human tissue was obtained from National Disease Research Interchange, University of California at San Francisco, and Southeast Tissue Alliance. We thank Dr. Michael Liebschner (Rice University) for μCT imaging of the specimens. Additionally, Jenni Buckley, John Christensen, and Prem Nagarathnam performed various aspects of the mechanical testing, specimen preparation, and image processing. T.M.K. has a financial interest in O.N. Diagnostics, and both he and the company may benefit from the results of this research.

REFERENCES

1. Schuit SC, van der Klift M, Weel AE, de Laet CE, Burger H, Seeman E, Hofman A, Uitterlinden AG, van Leeuwen JP, Pols HA 2004 Fracture incidence and association with bone mineral density in elderly men and women: The Rotterdam Study. Bone **34:**195–202.
2. Cummings SR, Karpf DB, Harris F, Genant HK, Ensrud K, LaCroix AZ, Black DM 2002 Improvement in spine bone density and reduction in risk of vertebral fractures during treatment with antiresorptive drugs. Am J Med **112:**281–289.
3. Delmas PD, Seeman E 2004 Changes in bone mineral density explain little of the reduction in vertebral or nonvertebral fracture risk with anti-resorptive therapy. Bone **34:**599–604.
4. Heaney RP 2003 Is the paradigm shifting? Bone **33:**457–465.
5. Hernandez CJ, Keaveny TM 2006 A biomechanical perspective on bone quality. Bone **39:**1173–1181.
6. Goulet RW, Goldstein SA, Ciarelli MJ, Kuhn JL, Brown MB, Feldkamp LA 1994 The relationship between the structural and orthogonal compressive properties of trabecular bone. J Biomech **27:**375–389.
7. Hou FJ, Lang SM, Hoshaw SJ, Reimann DA, Fyhrie DP 1998 Human vertebral body apparent and hard tissue stiffness. J Biomech **31:**1009–1015.
8. Ulrich D, van Rietbergen B, Laib A, Rüegsegger P 1999 The ability of three-dimensional structural indices to reflect mechanical aspects of trabecular bone. Bone **25:**55–60.
9. Newitt DC, Majumdar S, van Rietbergen B, von Ingersleben G, Harris ST, Genant HK, Chesnut C, Garnero P, MacDonald B 2002 In vivo assessment of architecture and micro-finite element analysis derived indices of mechanical properties of trabecular bone in the radius. Osteoporos Int **13:**6–17.
10. Hansson T, Roos B 1981 The relation between bone mineral content, experimental compression fractures, and disc degeneration in lumbar vertebrae. Spine **6:**147–153.
11. Cody DD, Goldstein SA, Flynn MJ, Brown EB 1991 Correlations between vertebral regional bone mineral density (rBMD) and whole bone fracture load. Spine **16:**146–154.
12. Singer K, Edmondston S, Day R, Breidahl P, Price R 1995 Prediction of thoracic and lumbar vertebral body compressive strength—correlations with bone mineral density and vertebral region. Bone **17:**167–174.
13. Ebbesen EN, Thomsen JS, Beck-Nielsen H, Nepper-Rasmussen HJ, Mosekilde L 1999 Lumbar vertebral body compressive strength evaluated by dual-energy X-ray absorptiometry, quantitative computed tomography, and ashing. Bone **25:**713–724.
14. Eswaran SK, Gupta A, Adams MF, Keaveny TM 2006 Cortical and trabecular load sharing in the human vertebral body. J Bone Miner Res **21:**307–314.
15. Edmondston SJ, Singer KP, Day RE, Price RI, Breidahl PD 1997 Ex vivo estimation of thoracolumbar vertebral body compressive strength: The relative contributions of bone densitometry and vertebral morphometry. Osteoporos Int **7:**142–148.
16. Banse X, Devogelaer JP, Munting E, Delloye C, Cornu O, Grynpas M 2001 Inhomogeneity of human vertebral cancellous bone: Systematic density and structure patterns inside the vertebral body. Bone **28:**563–571.
17. Hulme PA, Boyd SK, Ferguson SJ 2007 Regional variation in vertebral bone morphology and its contribution to vertebral fracture strength. Bone **41:**946–957.
18. Andresen R, Werner HJ, Schober HC 1998 Contribution of the cortical shell of vertebrae to mechanical behaviour of the lumbar vertebrae with implications for predicting fracture risk. Br J Radiol **71:**759–765.
19. Homminga J, Van-Rietbergen B, Lochmüller EM, Weinans H, Eckstein F, Huiskes R 2004 The osteoporotic vertebral structure is well adapted to the loads of daily life, but not to infrequent ''error'' loads. Bone **34:**510–516.
20. Morgan EF, Bayraktar HH, Keaveny TM 2003 Trabecular bone modulus-density relationships depend on anatomic site. J Biomech **36:**897–904.
21. Müller R, Hannan M, Smith SY, Bauss F 2004 Intermittent ibandronate preserves bone quality and bone strength in the lumbar spine after 16 months of treatment in the ovariectomized cynomolgus monkey. J Bone Miner Res **19:**1787–1796.
22. Hildebrand T, Laib A, Müller R, Dequeker J, Rüegsegger P 1999 Direct three-dimensional morphometric analysis of human cancellous bone: Microstructural data from spine, femur, iliac crest, and calcaneus. J Bone Miner Res **14:**1167–1174.
23. Odgaard A, Gundersen HJ 1993 Quantification of connectivity in cancellous bone, with special emphasis on 3-D reconstructions. Bone **14:**173–182.
24. Eriksson SA, Isberg BO, Lindgren JU 1989 Prediction of vertebral strength by dual photon absorptiometry and quantitative computed tomography. Calcif Tissue Int **44:**243–250.
25. Faulkner KG, Cann CE, Hasegawa BH 1991 Effect of bone distribution on vertebral strength: Assessment with patient-specific nonlinear finite element analysis. Radiology **179:** 669–674.
26. Kopperdahl DL, Pearlman JL, Keaveny TM 2000 Biomechanical consequences of an isolated overload on the human vertebral body. J Orthop Res **18:**685–690.
27. Buckley JM, Loo K, Motherway J 2007 Comparison of quantitative computed tomography-based measures in predicting vertebral compressive strength. Bone **40:**767–774.

28. Carter DR, Hayes WC 1977 The compressive behavior of bone as a two-phase porous structure. J Bone Joint Surg Am **59:**954–962.
29. Linde F, Nørgaard P, Hvid I, Odgaard A, Søballe K 1991 Mechanical properties of trabecular bone. Dependency on strain rate. J Biomech **24:**803–809.
30. Eswaran SK, Bayraktar HH, Adams MF, Gupta A, Hoffman PF, Lee DC, Papadopoulos P, Keaveny TM 2007 The micromechanics of cortical shell removal in the human vertebral body. Comput Methods Appl Mech Eng **196:**3025–3032.
31. Eswaran SK, Gupta A, Keaveny TM 2007 Locations of bone tissue at high risk of initial failure during compressive loading of the human vertebral body. Bone **41:**733–739.
32. Mosekilde L 1993 Vertebral structure and strength in vivo and in vitro. Calcif Tissue Int **53:**S121–S126.
33. Silva MJ, Wang C, Keaveny TM, Hayes WC 1994 Direct and computed tomography thickness measurements of the human lumbar vertebral shell and endplate. Bone **15:**409–414.
34. Roy ME, Rho JY, Tsui TY, Evans ND, Pharr GM 1999 Mechanical and morphological variation of the human lumbar vertebral cortical and trabecular bone. J Biomed Mater Res **44:**191–197.
35. Lewis G 1997 Properties of acrylic bone cement: State of the art review. J Biomed Mater Res **38:**155–182.
36. Adams MF, Bayraktar HH, Keaveny TM, Papadopoulos P 2004 Ultrascalable implicit finite element analyses in solid mechanics with over a half a billion degrees of freedom. ACM/IEEE Proceedings of SC2004: High Performance Networking and Computing, Pittsburgh, PA, USA.
37. Crawford RP, Cann CE, Keaveny TM 2003 Finite element models predict in vitro vertebral body compressive strength better than quantitative computed tomography. Bone **33:**744–750.
38. MacNeil JA, Boyd SK 2007 Accuracy of high-resolution peripheral quantitative computed tomography for measurement of bone quality. Med Eng Phys **29:**1096–1105.
39. Kopperdahl DL, Morgan EF, Keaveny TM 2002 Quantitative computed tomography estimates of the mechanical properties of human vertebral trabecular bone. J Orthop Res **20:**801–805.
40. Cann CE, Genant HK, Kolb FO, Ettinger B 1985 Quantitative computed tomography for prediction of vertebral fracture risk. Bone **6:**1–7.
41. Bay BK, Yerby SA, McLain RF, Toh E 1999 Measurement of strain distributions within vertebral body sections by texture correlation. Spine **24:**10–17.
42. Crawford RP, Keaveny TM 2004 Relationship between axial and bending behaviors of the human thoracolumbar vertebra. Spine **29:**2248–2255.
43. Roschger P, Gupta HS, Berzlanovich A, Ittner G, Dempster DW, Fratzl P, Cosman F, Parisien M, Lindsay R, Nieves JW, Klaushofer K 2003 Constant mineralization density distribution in cancellous human bone. Bone **32:**316–323.
44. Ito M, Ikeda K, Nishiguchi M, Shindo H, Uetani M, Hosoi T, Orimo H 2005 Multi-detector row CT imaging of vertebral microstructure for evaluation of fracture risk. J Bone Miner Res **20:**1828–1836.
45. Eckstein F, Matsuura M, Kuhn V, Priemel M, Müller R, Link TM, Lochmüller EM 2007 Sex differences of human trabecular bone microstructure in aging are site-dependent. J Bone Miner Res **22:**817–824.
46. Melton LJ III, Riggs BL, Keaveny TM, Achenbach SJ, Hoffmann PF, Camp JJ, Rouleau PA, Bouxsein ML, Amin S, Atkinson EJ, Robb RA, Khosla S 2007 Structural determinants of vertebral fracture risk. J Bone Miner Res **22:**1885–1892.
47. Sornay-Rendu E, Boutroy S, Munoz F, Delmas PD 2007 Alterations of cortical and trabecular architecture are associated with fractures in postmenopausal women, partially independent of decreased BMD measured by DXA: The OFELY study. J Bone Miner Res **22:**425–433.
48. Lochmüller EM, Pöschl K, Würstlin L, Matsuura M, Müller R, Link TM, Eckstein F 2008 Does thoracic or lumbar spine bone architecture predict vertebral failure strength more accurately than density? Osteoporos Int **19:**537–545.
49. Snyder BD, Piazza S, Edwards WT, Hayes WC 1993 Role of trabecular morphology in the etiology of age-related vertebral fractures. Calcif Tissue Int **53S:**S14–S22.
50. Rockoff SD, Sweet E, Bleustein J 1969 The relative contribution of trabecular and cortical bone to the strength of human lumbar vertebrae. Calcif Tissue Res **3:**163–175.
51. Yoganandan N, Myklebust JB, Cusick JF, Wilson CR, Sances A 1988 Functional biomechanics of the thoracolumbar vertebral cortex. Clin Biomech **3:**11–18.
52. Liu XS, Bevill G, Keaveny TM, Sajda P, Guo XE 2008 Micromechanical analyses of vertebral trabecular bone based on individual trabeculae segmentation of plates and rods. J Biomech **42:**249–256.

Received in original form July 25, 2008; revised form January 15, 2009; accepted March 25, 2009.